

RESONANT IMPURITY SCATTERING IN HEAVY FERMION SUPERCONDUCTORS

P. Hirschfeld *

Physik-Department, Technische Universität München, D-8046 Garching, Federal Republic of Germany

D. Vollhardt **

Max-Planck-Institut für Physik und Astrophysik, Werner-Heisenberg Institut für Physik, Föhringer Ring 6, D-8000 München, Federal Republic of Germany

P. Wölfle ***

Physik-Department, Technische Universität München, D-8046 Garching, Federal Republic of Germany

The effect of resonant impurity scattering on the properties of superconducting heavy fermion compounds proposed recently by Pethick and Pines is investigated within a self-consistent theory of pair-breaking. We discuss the thermodynamic and transport properties of axial and polar type order parameters for a range of impurity concentrations and scattering phase shifts. The results for the polar state with impurity concentrations $n_i \sim 10^{-4}$ and phase shifts δ_0 close to the unitarity limit $\pi/2$ appear to give a good description of data on UPt_3 . Unusual behavior is predicted to occur in a gapless regime below a temperature $T_0 \sim T_c \cdot (n_i T_f / T_c)^{1/2}$.

The low temperature properties of the so-called heavy fermion superconductors^{1,2,3} UPt_3 , UBe_{13} and $CeCu_2Si_2$ appear to obey power laws in temperature in contrast to the exponential behavior familiar from the usual BCS theory. This and certain notions of the electron correlations in a heavy fermion system^{4,5} have led to the suggestion that these materials may be "unconventional", non s-wave superconductors. However, early model calculations exploring the possibility of anisotropic p-wave superconductivity analogous to the superfluidity in 3He have only met with partial success.

For example, the evaluation of (orientation averaged) transport coefficients in the Born approximation valid in normal superconductors yields invariably the same temperature dependence as in the normal state, independent of the gap structure. This arises because the product of the density of states $N(E)$ and the transport time $\tau(E)$ is energy independent in this approximation⁶. By contrast, experimentally these coefficients vanish with a higher power of T at low temperature.

A possible explanation of the transport data has been proposed recently by Pethick

and Pines⁷, who argue that due to the large effective mass any charged impurity potential is strongly screened, such that the scattering is essentially s-wave. In this case the Friedel sum rule implies that the scattering phase shift $\delta_0 \sim \pi q / N_f$, where q is the charge of the impurity and N_f is the level degeneracy of the scattering electrons. For $q=1$ and $N_f=2$ (only spin degeneracy) the scattering is near the unitarity limit $\delta_0 = \pi/2$. It has also been suggested⁸ that in a Kondo lattice model of a heavy fermion system an impurity representing a missing Kondo ion is associated with a Kondo phase shift of $\delta_0 = \pi/2$.

Resonance scattering implies that the transport relaxation rates are dramatically enhanced at low energy such that the transport coefficients are substantially reduced compared to the normal state, as observed experimentally. On the other hand, non-magnetic impurities cause pairbreaking in anisotropic, odd- and even-parity superconductors, in contrast to ordinary s-wave superconductors. Within the Born approximation these effects are negligible at the small concentrations we consider here⁹. However, resonant impurity scattering leads to significant changes in the BCS single-particle properties, such that a self-consistent treatment is always necessary.

In this paper we explore the consequences of this effect. Very recently the same problem was treated independently by Schmitt-Rink, Miyake and Varma⁶ (see also ref.10). A number of authors have considered the similar problem of Kondo impurities in usual superconductors, where one finds an impurity bound state in the

* Work partially supported by Deutsche Forschungsgemeinschaft

** Heisenberg - Fellow of the Deutsche Forschungsgemeinschaft

*** Also at Max-Planck-Institut für Physik und Astrophysik, München, F.R.G.
Address after August 1986: Dept. of Physics, University of Florida, Gainesville, FL 32611

gap^{1,2}. We shall concentrate on the low energy (and, hence, low temperature) regime, where pairbreaking is of dominant importance. Furthermore, we investigate the rôle of scattering phase shifts δ_0 different from $\pi/2$. It turns out that small changes in δ_0 may lead to significantly different behavior. We also discuss the actual temperature dependence of various physical properties for temperatures up to T_c . We find that the power law energy dependences of the density of states and the mean free path do not automatically translate into equivalent power laws in the temperature dependences of the corresponding frequency integrated physical quantities. This modifies somewhat the conclusions drawn in ref. 8. At low temperatures, where such power laws are normally valid, a gapless behavior intervenes, while at higher temperatures the power laws are destroyed by the upper cutoff of frequency power laws at $\omega = \Delta_0$ and by the temperature dependence of the order parameter.

Within a single-site approximation the effect of potential scattering is given by the T-matrix, which obeys the equation

$$\underline{T} = \underline{K} + \underline{K} \underline{G} \underline{T} \quad (1)$$

Here \underline{T} , the K-matrix \underline{K} and \underline{G} are matrices in Nambu space. In particular \underline{K} may be approximated by its normal state limit $\underline{K} = K_N \underline{\tau}_3$, where $K_N = -\tan \delta_0$ (N_0 is the normal density of states), because it is determined by virtual excitation processes into states far from the Fermi surface which are weakly affected by pairing. The matrix \underline{G} is the momentum integrated Green's function, $\underline{G}(\omega) = (1/\pi N_0) \int \underline{G}(\vec{k}, \omega)$. The Green's function is determined self-consistently from the Dyson equation

$$(\omega \underline{\tau}_0 - \xi_k \underline{\tau}_3 - \underline{\Delta}_k - \underline{\Sigma}(\omega)) \underline{G}(\vec{k}, \omega) = \underline{\tau}_0, \quad (2)$$

where ξ_k is the quasiparticle energy, $\underline{\Delta}_k = \underline{\tau}_1(\Delta_k + \Delta_k^+)/2 + \underline{\tau}_2(\Delta_k - \Delta_k^+)/2$ and Δ_k^+ is the gap function (the spin dependence of Δ_k^+ is irrelevant for our discussion and will be omitted). Here $\underline{\tau}_1, \underline{\tau}_2, \underline{\tau}_3$ are the Pauli matrices and $\underline{\tau}_0$ is the unit matrix in Nambu space. $\underline{\Sigma}(\omega)$ is the impurity self-energy matrix, which is given in terms of the T-matrix by

$$\underline{\Sigma}(\omega) = n_1 \left(\frac{N}{V} \right) \underline{T}(\omega), \quad (3)$$

with n_1 the impurity concentration and (N/V) the electron density. In order to solve (1), (2) and (3) we expand all the matrix quantities as

$\underline{T} = \sum_{j=0}^3 \underline{T}_j \underline{\tau}_j$. The problem simplifies considerably if one makes use of (i) particle hole symmetry, which implies $G_3(\omega) = 0$ and (ii) the fact that $G_2(\omega) = 0$ for intrinsically real gap functions, i.e. $\Delta_k = e^{i\phi} |\Delta_k|$ with ϕ independent of \vec{k} . Moreover, for odd-parity pairing states and for most of the anisotropic even-parity states that have been defined within a group theoretical classification¹³, Δ_k changes sign under at least one of the following symmetry transformations (i) inversion, (ii) rotation by $\pi/2$ or π , (iii) reflection, such that $G_1 = 0$. Possible exceptions are certain singlet states in

hexagonal crystal symmetry, where $G_1 \neq 0$ on account of the hexagonal anisotropy of the Fermi surface (the singlet state with lines of nodes $\Delta_k \propto k_x k_y$ would be of this type). Keeping only G_0 and G_1 one finds the components of the self-energy as

$$\Sigma_0 = G_0 \Sigma_1 / G_1 = \Gamma \frac{G_0}{c^2 - G_0^2 + G_1^2} \quad (4)$$

where $\Gamma = (n_1/\pi N_0)(N/V)$ is the normal state scattering rate in the unitarity limit and $c = \cot \delta_0$ is a convenient measure of the scattering strength. Note that $c=0$ at resonance, whereas $c \gg 1$ corresponds to the weak scattering limit. The integrated Green's functions are given by

$$G_0(\omega) = i \left\langle \frac{\tilde{\omega}}{(\tilde{\omega}^2 - \Delta_k^2)^{1/2}} \right\rangle_{\vec{k}} \quad (5)$$

and a similar expression for G_1 , with $\tilde{\omega} = \omega - \Sigma_0$ replaced by $\Delta_k^+ - \Sigma_1$ in the numerator. Similarly the gap function is determined self-consistently from the gap equation

$$\Delta_k = -T \sum_{\omega_n} \sum_{\vec{k}'} V_{\vec{k}\vec{k}'} \frac{1}{2} \text{tr} [\underline{\tau}_1 \underline{G}(\vec{k}', \omega_n)], \quad (6)$$

where $V_{\vec{k}\vec{k}'}$ is the pair potential. Equations (1)-(6) provide a general framework for the self-consistent calculation of single-site impurity scattering in superconducting states with arbitrary anisotropic (real) order parameter. The generalization to complex gap parameters is straightforward. For simplification we shall put $G_1 = 0$ in the following, thus excluding certain even-parity states in hexagonal crystals.

In the normal state $G_0 = i$, and $\Sigma_0 = i\Gamma \sin^2 \delta_0 = i\Gamma_N$. The depression of T_c by potential scattering, which acts as pairbreaking mechanism for triplet or singlet anisotropic pairing, is given by the usual AG expression¹⁴, with the magnetic scattering rate replaced by Γ_N . The relevant dimensionless parameter ($\Gamma_N/2\pi T_c$) in the unitarity limit is roughly given by $(n_1 T_F/T_c)$ with n_1 the concentration of impurities. Assuming $T_F \sim 10^4 (m/m^*) T_c$, a concentration of several percent should be sufficient to destroy superconductivity. On the other hand given an estimated impurity concentration¹⁵ of nominally pure samples of $n_1 \sim 10^{-4}$, T_c should not be affected. The gap parameter is reduced in order Γ/T_c for small n_1 .

Whereas resonance scattering by a small number of impurities does not affect those thermodynamic quantities which involve integration over energies of order T_c or Δ , it does cause large changes in the low energy and low temperature behavior and in the transport properties in general. Thus we find that the density of states is finite at zero energy in an axial state ($\Delta_k = \Delta_0 \sin \theta_k$) provided the pair-breaking parameter $\gamma = (\Gamma/\Delta_0)$ is sufficiently large, i.e. $\gamma > 2c^2/\pi$. For scattering in the unitarity limit $N(0)$ is finite for arbitrarily small concentration. In the polar state $N(0) > 0$ for all Γ, c . The dependence of $N(0)$ on γ and c is given for the axial state by

$$\frac{N(0)}{N_0} = \frac{u}{\tan u} = f_1(\gamma), \quad ,$$

and for the polar state by (7)

$$\frac{N(\omega)}{N_0} = \frac{y}{\sinh y} = f_2(y),$$

where y is the solution of $f_1^2(y) = \gamma y - c^2$. The region in frequency over which $N(\omega)$ is markedly different from the result for the pure state is roughly given by $\omega_c \sim \gamma^{1/2} \Delta_0$. Note that for frequencies $\omega > \omega_c$ self-consistency is essentially irrelevant. In fig. 1 we show the density of states for $\gamma = 0.01$ for the polar and axial states and various values of c . It is seen that the resonance peak centered at $\omega = 0$ for $c = 0$ moves to finite ω values as c increases. These results are strikingly different from the ones obtained in the Born approximation⁹.

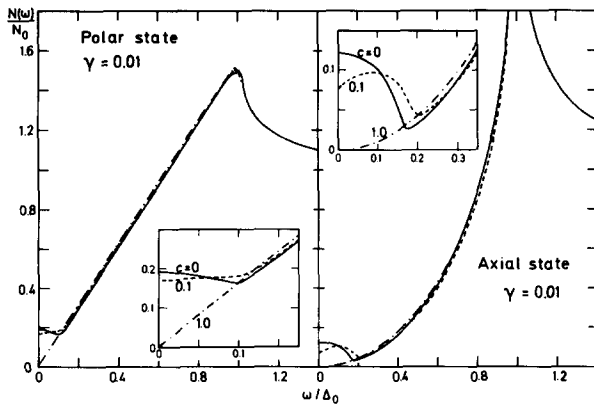


Fig. 1. Energy dependence of the density of states of the polar and axial states for a pair-breaking parameter of $\gamma = 0.01$ and different values of $c = \cot \delta_0$. The inserts illustrate the behavior in the low-energy, gapless region.

The specific heat C as a function of temperature reflects essentially the density of states. Thus the data on UPt_3 ¹⁶⁻¹⁹, which may be fitted by the law $C(T) = \alpha T + \beta T^2$ above $\sim 3T_c$ are compatible with our results for the polar state. If one extrapolates linearly to zero temperature while preserving entropy balance, C/T is finite at $T = 0$ ¹⁷, implying a finite density of states $N(0)$ corresponding to $\gamma \sim 0.03$ at $c = 0$. The comparison is shown in fig. 2, where $C(T)/T$ is plotted for $c = 0$ and 1 in the axial and polar state. The data for UPt_3 are more closely fitted by a pure axial state²⁰.

As pointed out by Pethick and Pines⁷, the transport properties are strongly affected by resonantly scattering impurities. In the unitarity limit the relaxation rate is found to be proportional to $1/G_0$ rather than G_0 as for weak scattering. Since the pairing correlations tend to force G_0 to zero in the limit of excitation energy $\omega \rightarrow 0$, the scattering at low energies ($\omega \ll \Delta_0$) is seen to be strongly enhanced, and the corresponding mean free path becomes very short. On the other hand, strong scattering means strong pair-breaking, such that eventually a gapless regime is reached at frequencies $\omega \sim \omega_c \sim \sqrt{\eta_1}$ (or correspondingly low temperatures). In this regime the

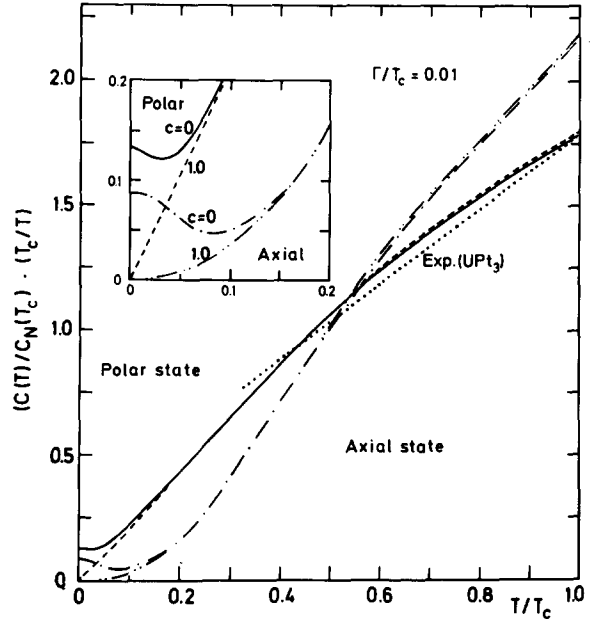


Fig. 2. Temperature dependence of the normalized specific heat $(C(T) \cdot T_c) / (C_n(T_c) \cdot T)$ for the polar and axial states for $c = 0$ and 1, with $\Gamma/T_c = .01$. The experimental results of ref. 18 on UPt_3 are indicated by a dotted line.

system behaves as in the normal state, albeit with reduced density of states. It is not to be expected that the transport properties follow a clean power law in temperature in the range above the gapless regime, which would be $T/T_c \gtrsim 0.1$ in currently available samples. As we will show, however, the behavior is sometimes accidentally close to a pure power law.

Straightforward generalization to anisotropic superconductors of the standard theory²¹ for the eigenvalues of the thermal conductivity tensor parallel and perpendicular to the gap axis yields

$$\frac{K_{\parallel}}{K_N(T_c)} = \frac{3}{2\pi^2} \frac{1}{T_c} \int_0^{\infty} d\omega \left(\frac{\omega}{T}\right)^2 \text{sech}^2 \frac{\omega}{2T} K_1(\omega) \quad (8)$$

where the dimensionless quantities K_1 are given by the angular averages over the Fermi surface:

$$K_1(\omega) = 3 \frac{N}{\text{Im}(\Sigma_0)} \langle \hat{p}_1^2 I(\omega; \Delta_p) \rangle_p \quad (9)$$

where

$$I(\omega; \Delta_p) = \frac{1}{2\text{Re}(\tilde{\omega})} \text{Re} \left\{ 2\sqrt{\tilde{\omega}^2 - \Delta_p^2} + \frac{|\tilde{\omega}|^2 - \tilde{\omega}^2}{\sqrt{\tilde{\omega}^2 - \Delta_p^2}} \right\} \quad (10)$$

and $\tilde{\omega} = \omega - \Sigma_0(\omega)$. In the region of not too low frequencies (temperatures) $\omega > \omega_c$, the renormalized complex frequency $\tilde{\omega}$ may be replaced by ω in (10). For the polar state one then finds in the unitarity limit for the components $K_{\parallel}(\omega) = (1 - x^2/4)K(\omega)$ and $K_{\perp} = (x^2/2)K(\omega)$, with $x = \omega/\Delta_0$, where

$$K(\omega) \approx \frac{3}{4} |G_0(\omega)|^2 = \frac{3x^2}{16} \left[\pi^2 + \ln^2 \left(\frac{1+\sqrt{1-x^2}}{1-\sqrt{1-x^2}} \right) \right] \quad (11)$$

is the trace of K_i . A numerical evaluation of $K(\omega)$ shows that to a good approximation $K(\omega) \approx 1.6(\omega/\Delta_0)$ for $0.2 \lesssim \omega/\Delta_0 \lesssim 1$, which leads to a T^2 power law of the thermal conductivity of a polycrystalline sample in the temperature range from 0.1 to 0.5 of T_c . A similar behavior has been obtained by Schmitt-Rink et al.⁸. At temperatures below $T_0 \sim \omega_c$ the thermal conductivity K_I should vary linearly with T as in the normal state, but reduced by a factor of $3\gamma/2$. The parallel component should change from a T^4 behavior at higher temperature to linear, the ratio to the normal state value being much smaller and given by $\kappa_{\parallel}(T)/\kappa_N(T) \approx 3\gamma y / \sinh^2 y$, where y is the solution of the transcendental equation given after eqn. (7). Near T_c , i.e. for $\Delta(T) \ll T$, one finds $\kappa_{\parallel}(T) - \kappa(T_c) \approx - (1/3 - 1/(3+p)) \Delta^3(T)$, where p is the exponent of the power law of $K_i(\omega)$. In fig.3 we show the theoretical result for the average thermal conductivity $\kappa = (1/3)\Sigma \kappa_i$ in an axial state and a polar state for two values of the scattering phase shift ($c=0$ and $c=1$). The low temperature experimental data¹⁸ for UPT₃, shown as the dotted line, are somewhat above the theoretical result for small c -values

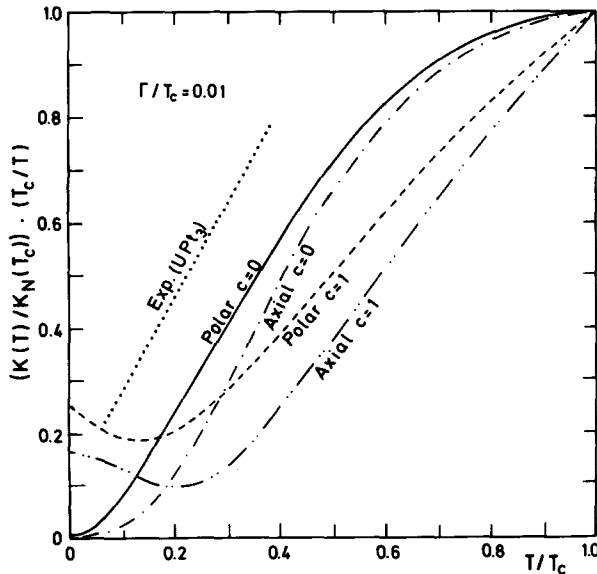


Fig. 3. Temperature dependence of the normalized thermal conductivity $(K(T) \cdot T_c) / (K_N(T_c) \cdot T)$ for the polar and axial states for $c=0$ and 1 , with $\Gamma/T_c = 0.01$. The low-temperature experimental results of ref. 18 for UPT₃ are indicated by the dotted line.

(note that $\kappa(0)/\kappa_N(0)$ approaches the limiting values $1/2$ and $1/3$ for the polar and axial states in the weak-scattering limit). We have tried various values of γ and c , but in no case do we find a substantially better fit over the entire temperature range. Better agreement

with the data would presumably obtain for a gap function with additional points and/or lines of nodes, which would enhance $\kappa(T)$ at low T .

In the hydrodynamic regime ($\omega\tau \ll 1$) the absorption of ultrasound of polarization e_i propagating along direction q_j is given by²²

$$\alpha_{ij}(T)/\alpha_N(T_c) = \frac{1}{2T} \int_0^{\omega} d\omega' \text{sech}^2 \frac{\omega'}{2T} A_{ij}(\omega'), \quad (12)$$

where α_N is the attenuation coefficient in the normal state and

$$A_{ij}(\omega) = \frac{1}{\langle \pi_{ij}^2 \rangle_{\hat{p}}} \frac{\Gamma_N}{\text{Im}(\Sigma_0)} \langle \pi_{ij}^2 I(\omega, \Delta_p) \rangle_{\hat{p}} \quad (13)$$

with $\pi_{ij} = \hat{p}_i \hat{p}_j - \delta_{ij}/3$ and I given by (10). In the frequency regime $\omega > \omega_c$ we find for a polar state in the unitarity limit ($c=0$, axis along z):

$$\begin{aligned} A_{xy} &\approx \frac{15}{16} \left(1 - \frac{x^2}{2} + \frac{x^4}{8} \right) |G_0|^2, \\ A_{xz} &\approx \frac{15}{16} \left(1 - \frac{x^2}{2} \right) x^2 |G_0|^2, \\ A_{xx} &\approx \frac{5}{64} \left(11 - \frac{15}{2} x^2 + \frac{27}{8} x^4 \right) |G_0|^2, \\ A_{zz} &\approx \frac{5}{8} \left(1 - \frac{3}{2} x^2 + \frac{3}{8} x^4 \right) |G_0|^2, \end{aligned} \quad (14)$$

which leads to approximate power laws $A_{xy}, A_{xx}, A_{zz} \approx \omega$ and $A_{xz} \approx \omega^3$ in the frequency range $0.1 \lesssim \omega/\omega_c \lesssim 1$. In fig. 4 the four components $\alpha_{xx}, \alpha_{xy}, \alpha_{xz}$ and α_{zz} are plotted as functions of temperature for a polar state with axis along z . The strikingly linear

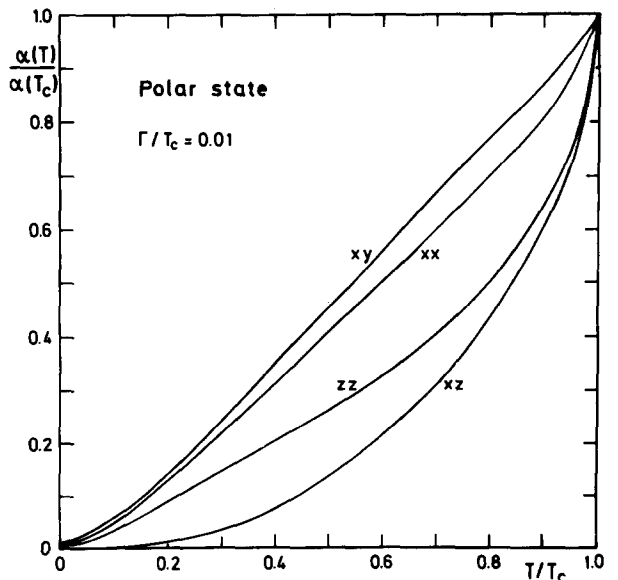


Fig. 4. Temperature dependence of the normalized sound attenuation $\alpha(T)/\alpha(T_c)$ in the polar state for various directions of propagation and polarization ($c=0, \Gamma/T_c=0.01$).

behavior of α_{xy} up to T_c is in good agreement with transverse ultrasound experiments²³ on UPT₃ for \hat{e} and \hat{q} in the basal plane of the hexagonal crystal. Furthermore, the calculated α_{xz} is compatible with the observed T^3 dependence²³ of α for \hat{q} in the basal plane and \hat{e} parallel to the c-axis of the hexagonal crystal. A T^3 behavior has also been observed for $\hat{q}\hat{e}$ and \hat{e} in the basal plane²⁴. These findings are consistent with the assumption of a polar phase for UPT₃. Concerning longitudinal sound there exist conflicting experimental results with power laws ranging from T^2 (ref. 25) to T^3 (ref. 24). Evaluating expression (12) for the polar state we find that α_{xx} and α_{zz} are not as close to a simple linear power law as may have been expected from the leading ω power in $A_{xx}(\omega)$ and $A_{zz}(\omega)$. Rather, α_{zz} varies roughly proportional to T^2 at higher temperatures and approaches a linear behavior only below $\sim 0.5 T_c$. This finding is also not inconsistent with experiment, in particular if one allows for somewhat higher impurity concentrations and/or finite values of c . It is possible that the apparent contradictions among the various longitudinal sound experiments on UPT₃ reflect differences in concentrations and kinds of impurities present.

For an axial state oriented along \hat{z} , we find approximately linear behavior above T_0 only for α_{zz} , whereas α_{xz} , α_{xx} , and in particular α_{xy} fall off rapidly below T_c . This is in contradiction to experiment. However, we

are not able to exclude an axial type state with nodes in the basal plane.

In conclusion, we find that by assuming (i) resonant scattering of the heavy electrons due to a low concentration of nonmagnetic impurities and (ii) a polar type superconducting state, we are able to provide a consistent description of the available experimental data for at least one of the heavy fermion compounds, namely UPT₃. This is in qualitative agreement with the conclusions of Schmitt-Rink et al.⁶. In particular, the ultrasound data appear to require a line of gap nodes, or possibly point nodes, in the basal plane of the hexagonal crystal. Since polar type odd-parity states do not appear to be allowed by symmetry,¹³ even-parity states should be considered. A possible candidate state is the intrinsically complex singlet state within the E_1 representation of D_6 , $\Delta_{\vec{r}} = k_z(k_x + i k_y)$, discussed by Volovik and Gorkov.¹³ Nevertheless, on the basis of our calculations, odd-parity states with point nodes in the basal plane (as, for example, states 3 and 4 for hexagonal symmetry in Blount's classification¹³) cannot be excluded with certainty. Further progress may be made by investigating more realistic model states.

Acknowledgements. We thank Dr. D. Einzel for advice on the numerical computations. We are grateful to Dr. C. M. Varma for providing us with a preprint of ref. 8 prior to publication.

References

- G.R. Stewart, Rev. Mod. Phys. **56**, 755 (1984)
- F. Steglich, in Theory of Heavy Fermions and Valence Fluctuations, eds. T. Kasuya and T. Saso, Springer Series in Solid State Sciences vol. 62, p. 23 (1985)
- Z. Fisk, H.R. Ott, T.M. Rice and J.L. Smith, preprint
- P.W. Anderson, Phys. Rev. **B30**, 1549 (1984)
- C.M. Varma, Comments in Solid State Physics **11**, 221 (1985)
- L. Coffey, T.M. Rice and K. Ueda, J. Phys. **C18**, L813 (1985)
- C.J. Pethick and D. Pines, preprint
- S. Schmitt-Rink, K. Miyake and C.M. Varma, preprint
- K. Ueda, T.M. Rice, in Theory of Heavy Fermions and Valence Fluctuations, eds. T. Kasuya and T. Saso, Springer Series in Solid State Sciences, vol. 62, p. 267 (1985)
- L.J. Buchholtz and G. Zwirnagl, Phys. Rev. **B 23**, 5788 (1981); these authors presented a self-consistent T-matrix theory for an isotropic, triplet superconductor (BW-state)
- K. Maki, Phys. Rev. **153**, 428 (1967); H. Shiba, Progr. Theor. Phys. **40**, 435 (1968)
- J. Zittartz, A. Bringer and E. Müller-Hartmann, Sol. St. Comm. **10**, 513 (1972)
- G.E. Volovik and L.P. Gorkov, ZhETF **88**, 1412 (1985) (Soviet Physics: JETP **61**, 843 (1985)); K. Ueda and T.M. Rice, Phys. Rev. **B31**, 7114 (1985); E.I. Blount, Phys. Rev. **B32**, 2935 (1985)
- A.A. Abrikosov and L.P. Gorkov, Zh. Eksp. Teor. Fiz. **39**, 1781 (1960) [Sov. Phys. JETP **12**, 1243 (1961)]
- H.R. Ott, private communication
- G.R. Stewart, Z. Fisk, J.O. Willis and J.L. Smith, Phys. Rev. Lett. **52**, 679 (1984)
- F. Steglich, U. Rauchschwalbe, U. Gottwick, H.M. Mayer, G. Sparn, N. Grewe, U. Poppe and J.J.M. Franse, J. Appl. Phys. **57**, 3054 (1985)
- A. Sulpice, P. Gandit, J. Chaussy, J. Flouquet, D. Jaccard, P. Lejay and J.L. Tholence, J. Low Temp. Phys. **62**, 39 (1986)
- J.J.M. Franse, A. Menovsky, A. de Visser, C.D. Bredl, U. Gottwick, W. Lieke, H.M. Mayer, U. Rauchschwalbe, G. Sparn and F. Steglich, Z. Physik **B59**, 15 (1985)
- H.R. Ott, H. Rudigier, T.M. Rice, K. Ueda, Z. Fisk and J.L. Smith, Phys. Rev. Lett. **52**, 1915 (1984)
- V. Ambegaokar and L. Tewordt, Phys. Rev. **134**, A805 (1964)
- L.P. Kadanoff and I.I. Falko, Phys. Rev. **136**, A1170 (1964)
- B.S. Shivaram, Y.H. Jeong, T.F. Rosenbaum and D.J. Hinks, preprint
- V. Müller, D. Maurer, E.W. Scheidt, C. Roth, K. Lüders, E. Bucher and H.E. Bömmel, Solid State Commun. **57**, 319 (1986)
- D.J. Bishop, C.M. Varma, B. Batlogg, E. Bucher, Z. Fisk and J.L. Smith, Phys. Rev. Lett. **53**, 1009 (1984)